



Article

Bone Mass and Osteoblast Activity Are Sex-Dependent in Mice Lacking the Estrogen Receptor α in Chondrocytes and Osteoblast Progenitor Cells

Lena Steppe ¹ , Jasmin Bülow ¹, Jan Tuckermann ² , Anita Ignatius ¹ and Melanie Haffner-Luntzer ^{1,*}

¹ Institute of Orthopedic Research and Biomechanics, University Medical Center Ulm, 89081 Ulm, Germany; lena.steppe@uni-ulm.de (L.S.); jasmin.buelow@uni-ulm.de (J.B.); anita.ignatius@uni-ulm.de (A.I.)

² Institute of Comparative Molecular Endocrinology (CME), Ulm University, 89081 Ulm, Germany; jan.tuckermann@uni-ulm.de

* Correspondence: melanie.haffner-luntzer@uni-ulm.de

Abstract: While estrogen receptor alpha (ER α) is known to be important for bone development and homeostasis, its exact function during osteoblast differentiation remains unclear. Conditional deletion of ER α during specific stages of osteoblast differentiation revealed different bone phenotypes, which were also shown to be sex-dependent. Since hypertrophic chondrocytes can transdifferentiate into osteoblasts and substantially contribute to long-bone development, we aimed to investigate the effects of ER α deletion in both osteoblast and chondrocytes on bone development and structure. Therefore, we generated mice in which the ER α gene was inactivated via a *Runx2*-driven cyclic recombinase (ER $\alpha^{\text{fl/fl}}$; *Runx2*^{Cre}). We analyzed the bones of 3-month-old ER $\alpha^{\text{fl/fl}}$; *Runx2*^{Cre} mice by biomechanical testing, micro-computed tomography, and cellular parameters by histology. Male ER $\alpha^{\text{fl/fl}}$; *Runx2*^{Cre} mice displayed a significantly increased cortical bone mass and flexural rigidity of the femurs compared to age-matched controls with no active Cre-transgene (ER $\alpha^{\text{fl/fl}}$). By contrast, female ER $\alpha^{\text{fl/fl}}$; *Runx2*^{Cre} mice exhibited significant trabecular bone loss, whereas in cortical bone periosteal and endosteal diameters were reduced. Our results indicate that the ER α in osteoblast progenitors and hypertrophic chondrocytes differentially contributes to bone mass regulation in male and female mice and improves our understanding of ER α signaling in bone cells in vivo.

Keywords: bone; estrogen; receptor knockout; genetic animal model; sex steroids; osteoblasts; chondrocytes; biomechanics



Citation: Steppe, L.; Bülow, J.; Tuckermann, J.; Ignatius, A.; Haffner-Luntzer, M. Bone Mass and Osteoblast Activity Are Sex-Dependent in Mice Lacking the Estrogen Receptor α in Chondrocytes and Osteoblast Progenitor Cells. *Int. J. Mol. Sci.* **2022**, *23*, 2902. <https://doi.org/10.3390/ijms23052902>

Academic Editor: Giacomina Brunetti

Received: 16 February 2022

Accepted: 4 March 2022

Published: 7 March 2022

Corrected: 27 May 2022

Publisher's Note: MDPI stays neutral with regard to jurisdictional claims in published maps and institutional affiliations.



Copyright: © 2022 by the authors. Licensee MDPI, Basel, Switzerland. This article is an open access article distributed under the terms and conditions of the Creative Commons Attribution (CC BY) license (<https://creativecommons.org/licenses/by/4.0/>).

1. Introduction

Sex steroids are essential for skeletal development and regulate bone mass in both males and females [1]. During puberty, estrogen exerts suppressive effects on bone growth, whereas testosterone promotes periosteal bone formation resulting in greater bone size and a stronger skeleton in males [2]. Highlighting the important functions of both hormones on skeletal maintenance, declining levels of estrogen during menopause, and a reduction of both estrogen and androgens with increasing age in men are associated with bone loss and the development of osteoporosis [3–5]. The effects of estrogen on bone are mainly mediated via the two estrogen receptors (ERs), ER α and ER β , which can both be also activated by androgens after aromatization into estrogens [6,7]. In bone, ER α and ER β are expressed in chondrocytes, osteoblasts, osteocytes, and osteoclasts [8,9]. It is known that ER α is expressed at higher levels in cortical bone, whereas ER β is strongly expressed in cancellous bone [10]. Because ER β modulates the transcriptional activity of ER α and antagonizes many of ER α -driven effects [11,12], a “ying yang” relationship between both receptors is described [13]. ER α has become a major focus of research, since a human case report demonstrated that a point mutation in its gene resulted in osteoporosis and unfused growth plates in a 28-year-old man [14]. Furthermore, case reports from men

that suffer from an aromatase deficiency together with preclinical studies demonstrated the importance of estrogens for male skeletal homeostasis [15–18]. In bone, ER α is mainly mediating the actions of estrogen and is therefore considered as more important for skeletal homeostasis [19,20]. Regarding sex-specific differences of ER α expression, we showed that during bone healing, ER α expression is lower in the fracture callus of male mice, specifically in hypertrophic chondrocytes, shown by immunohistochemical stainings and gene expression analysis of the fractured femurs [21]. Furthermore, in the literature, it is reported that cultured human osteoblasts from men and women respond differentially to estrogen or ER α /ER β -specific agonists in a sex-specific manner [22,23]. These findings indicate that the expression levels of ER α /ER β as well as their response to its ligand estrogen might be sex-specific. For this reason, we focused on the sex-specific role of ER α on bone.

The crucial role of ERs in skeletal health and growth was further confirmed by preclinical studies using global ER α - (ER α -KO) or ER β -knockout (ER β -KO) mice. In females and males, ER α -KO resulted in shorter long bones, whereas ER β -KO showed no effects on longitudinal bone growth [16,24–26]. Additionally, ER α -KO mice displayed a decrease in cortical bone mineral density (BMD) and an increased trabecular bone volume in both sexes [27]. However, in a mouse line with a global deletion of the ER α , unspecific effects or compensatory mechanisms by the increased serum levels of testosterone [27] or the low expression levels of a chimeric truncated ER α isoform due to alternative splicing [28] cannot be ruled out. Therefore, cell-specific knockout models were generated using the Cre/loxP technology to elucidate the role of ER α on different stages of the osteoblast life cycle (Figure 1, Table 1). Under the control of different promoter genes particularly expressed by the respective cell type, the expression of a Cre-recombinase leads to a deletion of the ER α in this cell type.

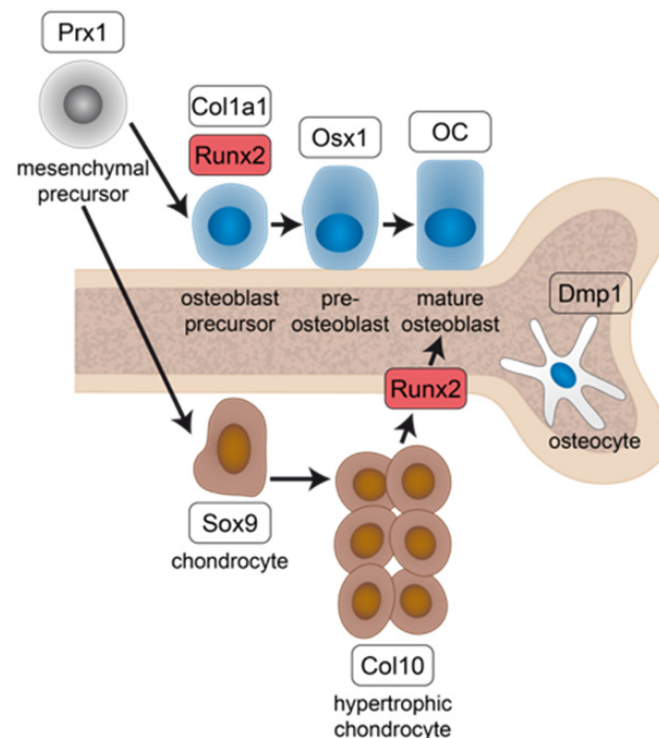


Figure 1. Schematic representation of osteoblast and chondrocyte lineage commitment from mesenchymal precursors, highlighting the progressive stages of differentiation with their associated characteristic genes (white boxes) that are used to develop osteoblast-specific Cre mouse lines (Table 1). Prx1 = paired-related homeobox 1; Runx2 = runt-related transcription factor 2; Osx1 = osterix; OC = osteocalcin; Dmp1 = dentin matrix protein 1; Sox9 = SRY-Box Transcription Factor 9; Col 10 = collagen type 10.

Table 1. Effects of osteoblast-specific ER α knockout models on cortical and trabecular bone in male and female mice.

Mouse Model	Females		Males	
	Cortical	Trabecular	Cortical	Trabecular
Osteoblast lineage				
ER α ^{fl/fl} <i>Prx1</i> -Cre [29]	↓ Ct. Th.	↔	↓ Ct. Th.	↔
ER α ^{fl/fl} <i>Runx2</i> -Cre [30]	N.a.	↓	N.a.	N.a.
ER α ^{fl/fl} <i>Runx2</i> -Cre	↔	↓	↑	↔
ER α ^{fl/fl} <i>Col1a1</i> -Cre [29]	↔	↔	↔	↔
ER α ^{fl/fl} <i>Osx1</i> -Cre [29]	↓	↔	N.a.	N.a.
ER α ^{fl/fl} <i>OC</i> -Cre [31]	↓	↓	↔	↔
ER α ^{fl/fl} <i>OC</i> -Cre [32]	↓	↓	N.a.	N.a.
ER α ^{fl/fl} <i>OC</i> -Cre [33] C57Bl/6 background	↓	↓	↑ Ct. Ar. ↑ Femoral length	↑ Tb. Th, BV/TV
ER α ^{fl/fl} <i>OC</i> -Cre [34]	↓	↓ Tb. BV	↔	↔
ER α ^{fl/fl} <i>Dmp1</i> -Cre [35]	↔	↔	↔	↓

↓ = reduced; ↑ = increased; ↔ = unaltered; N.a. = not available; Ct. Th. = cortical thickness, Ct. Ar. = cortical area; Tb. Th = trabecular thickness, BV/TV = relative bone volume; Tb. BV = trabecular bone volume.

Regarding the differentiation timeline of osteoblasts (Figure 1), first, *Prx1* is expressed by skeletal stem cells followed by *Runx2*, which is upregulated in osteoblastic precursors together with *Col1a1* [36]. When these precursors further differentiate, osterix (*Osx1*) is upregulated in pre-osteoblasts which then become mature osteoblasts, expressing high levels of osteocalcin (*OC*). *Dmp1* is mainly expressed by osteocytes. ER α deletion in skeletal stem cells (*Prx1*-Cre) resulted in a reduction of cortical bone mass and BMD in both sexes, whereas the trabecular bone mass was unchanged [29]. When ER α was deleted in pre-osteoblasts (*Osx1*-Cre), female mice displayed a reduced cortical thickness. A deletion of the ER α during the matrix maturation phase in osteoblasts via the *Col1a1*-Cre model [29] had no effect on the bone phenotype, neither in male nor in female mice. However, ER α deletion in mature osteoblasts and osteocytes (*OC*-Cre) resulted in a reduction of cortical and trabecular bone mass in females but not in males [32–34].

Taken together, these studies have established that bone development is regulated by ER α in osteoblastic cells. Thereby, ER α -mediated effects are dependent on the osteoblast differentiation stage and on the sex [32–34]. However, these studies did not take into account that hypertrophic chondrocytes can undergo transdifferentiation into osteoblasts [37,38], which essentially contributes to bone formation in long bones [39,40]. Therefore, here we investigated the role of ER α in both osteoblast lineage-specific cells and hypertrophic chondrocytes by using the *Runx2*-Cre mouse model. The transcription factor *Runx2* is essential for driving osteoblastogenesis and is expressed in hypertrophic chondrocytes, eventually transdifferentiating into osteoblasts (Figure 1) [41–43]. We crossbred *Runx2*-Cre with ER α floxed mice (ER α ^{fl/fl}) and analyzed the bone phenotype in both male and female mice to provide further insights into the regulatory functions of ER α in bone development.

We analyzed bone strength of male and female 3-month-old ER α ^{fl/fl}; *Runx2*^{Cre} mice by biomechanical testing, bone mass and structure by μ CT, and cellular parameters by histology. In male ER α ^{fl/fl}; *Runx2*^{Cre} mice, bone strength and cortical thickness were significantly increased compared to age-matched floxed control littermates with no active Cre-transgene (ER α ^{fl/fl}). In addition, the periosteal diameter and the moment of inertia were found to be significantly increased, whereas the ER α knockout had no effect on trabecular bone. By contrast, female ER α ^{fl/fl}; *Runx2*^{Cre} mice exhibited significant trabecular bone loss, whereas the cortical bone was mainly unaffected. Our results indicate a sex-specific role of the

ER α in osteoblast progenitors and hypertrophic chondrocytes on bone mass in male and female mice.

2. Results

2.1. Influence of ER α Deletion in Osteoblast Progenitors on Bone in Male Mice

The femur lengths of male ER $\alpha^{fl/fl}; Runx2^{Cre}$ mice were not different compared to ER $\alpha^{fl/fl}$ control animals (Figure 2A). To evaluate the flexural rigidity of the femurs and the bone structure of ER $\alpha^{fl/fl}; Runx2^{Cre}$ mice, biomechanical testing and μ CT analyses were performed. The ER $\alpha^{fl/fl}; Runx2^{Cre}$ males displayed a significant increased flexural rigidity of the femurs compared to their control littermates (Figure 2B), resulting from a significantly higher moment of inertia and from a significantly increased cortical TMD and thickness (Figure 2C–E). The periosteal bone diameter was significantly increased in ER $\alpha^{fl/fl}; Runx2^{Cre}$ mice, whereas the endosteal diameter was unchanged between both genotypes (Figure 2F,G). In the trabecular compartment, all analyzed bone parameters including BV/TV, trabecular number, thickness, and separation, as well as trabecular BMD, were unaltered (Figure 2H–L).

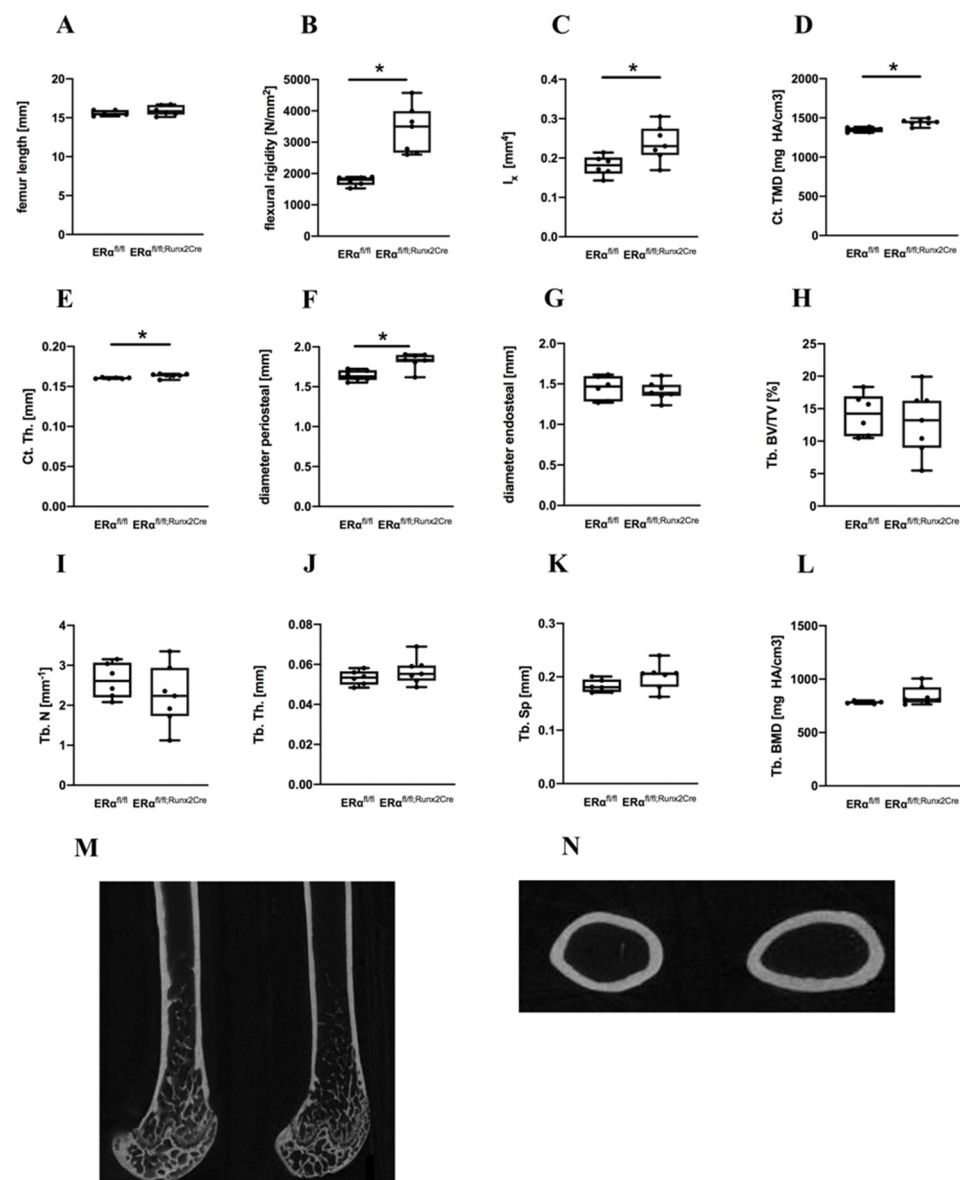


Figure 2. Bone-specific parameters of male ER $\alpha^{fl/fl}$ and ER $\alpha^{fl/fl}; Runx2^{Cre}$ mice. (A) Femur length; (B) bending stiffness of the right femur; (C) moment of inertia; (D) cortical tissue mineral density (Ct. TMD);

(E) cortical thickness (Ct. Th.); (F) diameter periosteal; and (G) diameter endosteal; (H) trabecular bone volume per tissue volume (Tb. BV/TV) (I) trabecular number (Tb. N). (J) Trabecular thickness (Tb. Th.); (K) trabecular separation (Tb. Sp). (L) Trabecular bone mineral density (Tb. BMD). (M) Representative μ CT reconstructions of the right femurs representing the bones of $ER\alpha^{fl/fl}$ mice (left panel) and of $ER\alpha^{fl/fl}; Runx2^{Cre}$ mice (right panel). (N) Representative cross-sectional μ CT images of $ER\alpha^{fl/fl}$ mice (left panel) and $ER\alpha^{fl/fl}; Runx2^{Cre}$ mice (right panel). Data are shown as box-and-whisker plot (with median and interquartile range) from maximum to minimum, showing all data points. * Indicates significant effects with $p \leq 0.05$.

Histomorphometric analyses of the metaphyseal region demonstrated that trabecular osteoblast number and surface were not affected by the $ER\alpha$ knockout (Figure 3). Similarly, trabecular osteoclast number and surface, as well as cortical osteocyte number, were unaltered (Figure 3). At the growth plate, osteoclast number as well as growth plate thickness were unchanged between both genotypes (Figure S1). Taken together, these results suggest that the deletion of $ER\alpha$ provoked an anabolic effect on the cortical bone of male mice.

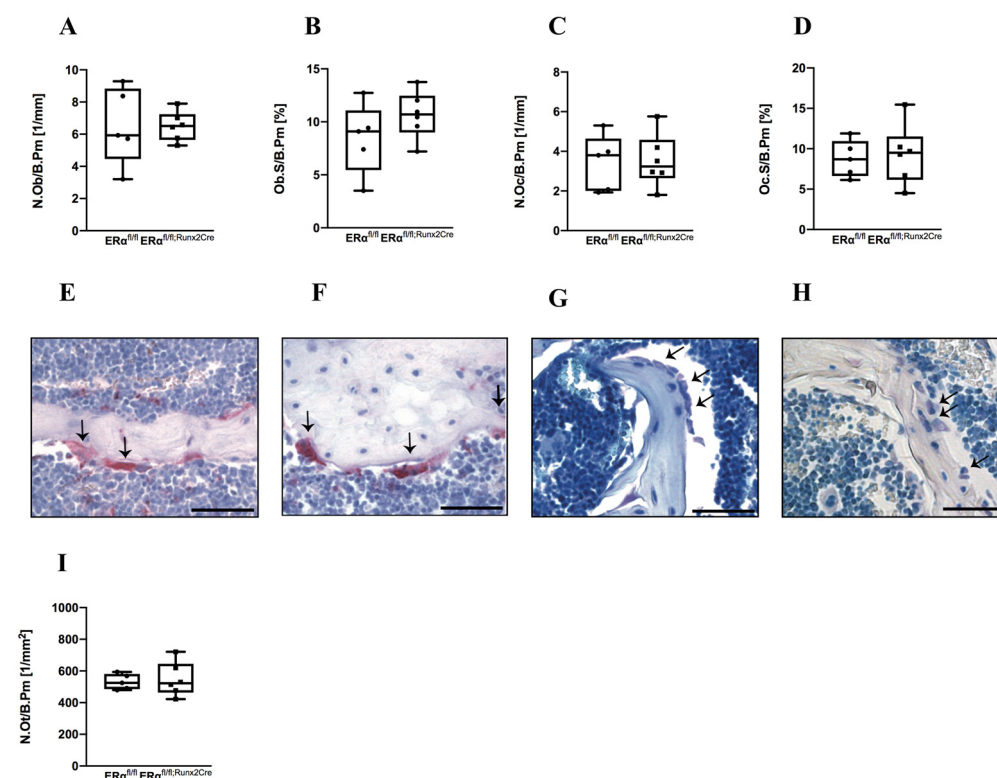


Figure 3. Histomorphometrical analysis of male $ER\alpha^{fl/fl}$ and $ER\alpha^{fl/fl}; Runx2^{Cre}$ mice. Representative paraffin sections of femora were stained with TRAP or Toluidine blue and histomorphometrical analysis was performed to determine (A) number of osteoblasts per bone perimeter (N.Ob/B.Pm), (B) osteoblast surface per bone surface (Ob.S/B.Pm), (C) number of osteoclasts per bone perimeter (N.Oc/B.Pm), and (D) osteoclast surface per bone surface (Oc.S/B.Pm). Representative images of TRAP-stained sections from (E) $ER\alpha^{fl/fl}$ mice or (F) $ER\alpha^{fl/fl}; Runx2^{Cre}$ mice as well as Toluidine blue-stained sections from (G) $ER\alpha^{fl/fl}$ mice or (H) $ER\alpha^{fl/fl}; Runx2^{Cre}$ mice. (I) Number of osteocytes per bone perimeter (N.Ot/B.Pm). Scale bar = 50 μ m. Data are shown as box-and-whisker plot (with median and interquartile range) from maximum to minimum, showing all data points.

2.2. Influence of $ER\alpha$ Deletion in Osteoblast Progenitors on Bone in Female Mice

In contrast to male $ER\alpha^{fl/fl}; Runx2^{Cre}$ mice, the femur lengths, flexural rigidity and the moment of inertia did not significantly differ in female $ER\alpha^{fl/fl}; Runx2^{Cre}$ mice compared to control animals (Figure 4A–C). Periosteal and endosteal diameters of the femurs were sig-

nificantly reduced in female $ER\alpha^{fl/fl}; Runx2^{Cre}$ mice, whereas the cortical TMD and thickness were unaltered (Figure 4D–G).

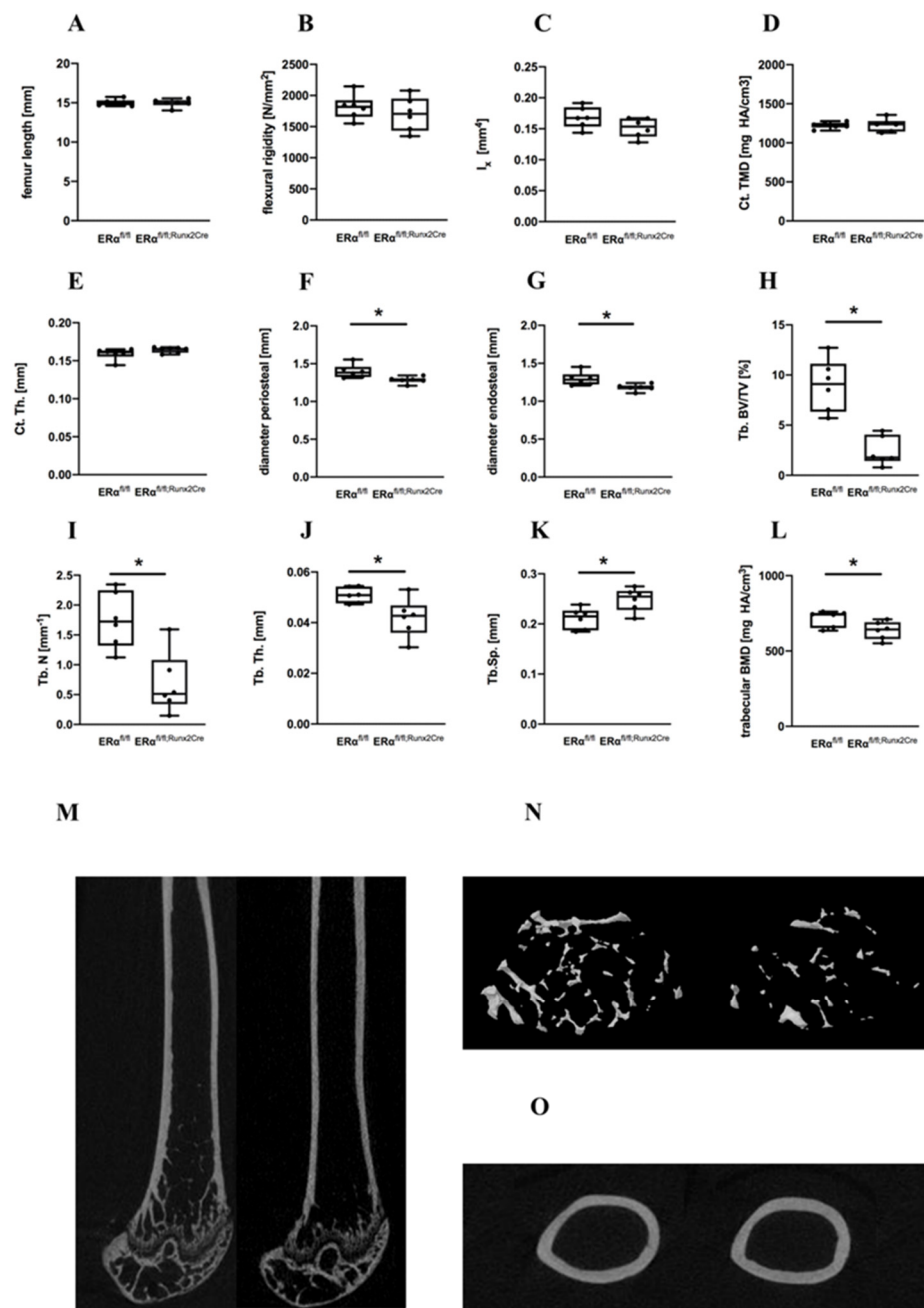


Figure 4. Bone-specific parameters of female $ER\alpha^{fl/fl}$ and $ER\alpha^{fl/fl}; Runx2^{Cre}$ mice. (A) Femur length; (B) bending stiffness of the right femur; (C) moment of inertia; (D) cortical tissue mineral density (Ct. TMD); (E) cortical thickness (Ct. Th.); (F) diameter periosteal; and (G) diameter endosteal; (H) trabecular bone volume per tissue volume (Tb. BV/TV) (I) trabecular number (Tb. N); (J) Trabecular thickness (Tb. Th.); (K) trabecular separation (Tb. Sp.); (L) trabecular bone mineral density (Tb. BMD). (M) Representative μ CT reconstructions of the right femora representing the bones of $ER\alpha^{fl/fl}$ mice (left panel) and of $ER\alpha^{fl/fl}; Runx2^{Cre}$ mice (right panel). (N) Representative μ CT images of trabecular bone microarchitecture in the distal femurs of $ER\alpha^{fl/fl}$ mice (left panel) and $ER\alpha^{fl/fl}; Runx2^{Cre}$ mice (right panel). (O) Representative cross-sectional μ CT images of $ER\alpha^{fl/fl}$ mice (left panel) and $ER\alpha^{fl/fl}; Runx2^{Cre}$ mice (right panel). Data are shown as box-and-whisker plot (with median and interquartile range) from maximum to minimum, showing all data points. * Indicates significant effects with $p \leq 0.05$.

In trabecular bone, the lack of the ER α in female mice led to severely reduced BV/TV, BMD, trabecular number, and thickness (Figure 4H–J,L,N and Figure S2 for epiphyseal bone). Consistently, trabecular separation was significantly increased in ER $\alpha^{fl/fl}; Runx2^{Cre}$ animals in comparison to their ER $\alpha^{fl/fl}$ littermates (Figure 4K). Furthermore, a significant reduction of the osteoblast number and surface in the trabecular bone was observed in female ER $\alpha^{fl/fl}; Runx2^{Cre}$ mice, whereas osteoclast number and surface were unaltered (Figure 5A–H). In addition, we found a significantly reduced osteocyte number per bone area in the cortical bone of ER $\alpha^{fl/fl}; Runx2^{Cre}$ animals (Figure 5I). Furthermore, at the growth plate, osteoclast number and growth plate thickness were not affected by the knockout (Figure S1). Osteogenic differentiation experiments of primary osteoblasts cultures isolated from both genotypes revealed a significantly diminished osteogenic differentiation ability of cells derived from ER $\alpha^{fl/fl}; Runx2^{Cre}$ animals shown by a significantly lower gene expression of alkaline phosphatase (*AP*), osteocalcin (*OC*), bone sialoprotein (*BSP*), and runt-related transcription factor-2 (*Runx2*) in vitro and shown by weaker AP stainings (Figure 5J–Q). Collectively, these findings indicate that female ER $\alpha^{fl/fl}; Runx2^{Cre}$ animals exhibited a reduced trabecular bone mass and altered cortical bone architecture based on a reduced osteoblast differentiation.

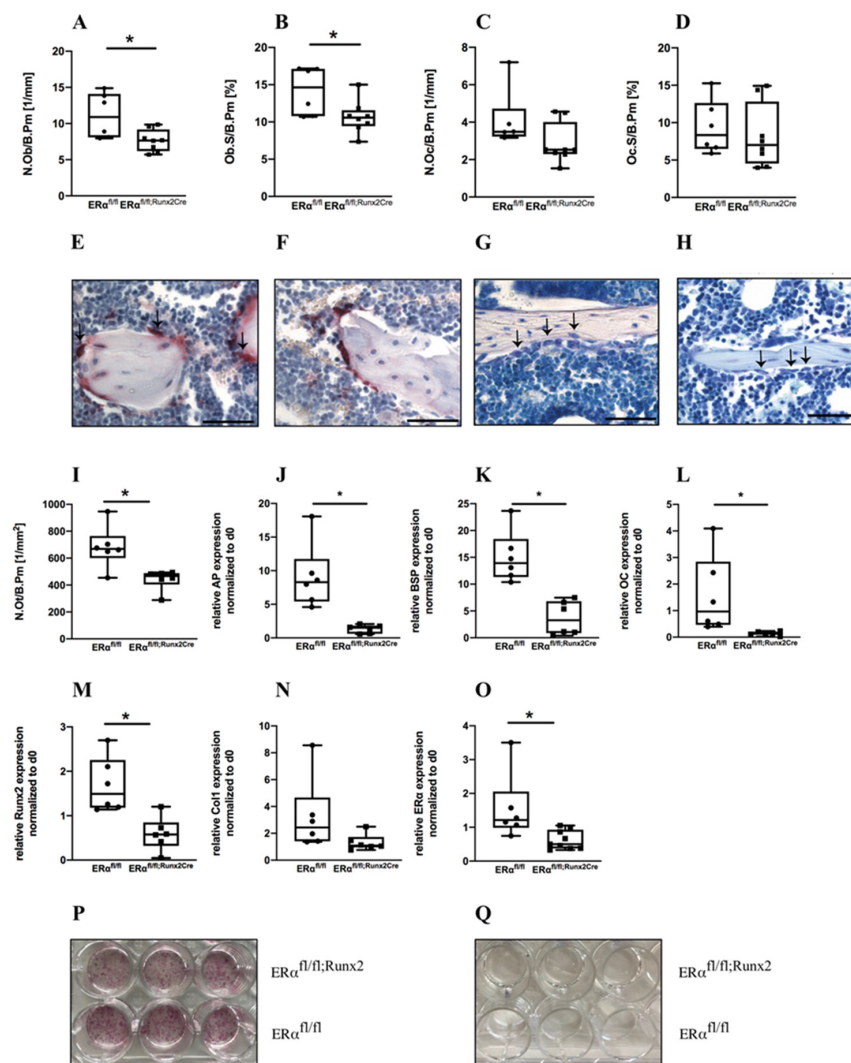


Figure 5. Histomorphometrical analysis of female ER $\alpha^{fl/fl}$ and ER $\alpha^{fl/fl}; Runx2^{Cre}$ mice and differentiation ability of isolated primary osteoblasts. Representative paraffin sections of femurs were stained with TRAP or Toluidine blue and histomorphometrical analysis was performed to determine (A) number of osteoblasts per bone perimeter (N.Ob/B.Pm); (B) osteoblast surface per bone surface

(ObS/B.Pm); (C) number of osteoclasts per bone perimeter (N.Oc/B.Pm); and (D) osteoclast surface per bone surface (OcS/B.Pm). Representative images of TRAP-stained sections from (E) ER $\alpha^{fl/fl}$ mice or (F) ER $\alpha^{fl/fl}; Runx2^{Cre}$ mice as well as Toluidine blue-stained sections from (G) ER $\alpha^{fl/fl}$ mice or (H) ER $\alpha^{fl/fl}; Runx2^{Cre}$ mice. (I) Number of osteocytes per bone perimeter (N.Ot/B.Pm). Primary osteoblasts were isolated from both ER $\alpha^{fl/fl}$ and ER $\alpha^{fl/fl}; Runx2^{Cre}$ mice and relative AP expression was determined with (J) qPCR and by (P,Q) AP stainings in either differentiation medium at d10 (P) or control medium at d0 (Q). Relative expression of (K) BSP, (L) OC, (M) Runx2, (N) Col1, and (O) ER α was determined with qPCR. Scale bar = 50 μ m. Data are shown as box-and-whisker plot (with median and interquartile range) from maximum to minimum, showing all data points. * Indicates significant effects with $p \leq 0.05$.

3. Discussion

In the present study, we aimed to examine whether ER α signaling in osteoblast lineage-specific cells and hypertrophic chondrocytes are required for bone formation and development. To this end, mice with a deletion of the ER α in both cell types were generated by breeding *Runx2*-Cre and ER α floxed mice. The *Runx2*-Cre model allows to study the role of ER α not only in osteoblast progenitor cells directly derived from skeletal stem cells, but also in hypertrophic chondrocytes eventually transdifferentiating into osteoblasts during long bone development.

In male ER $\alpha^{fl/fl}; Runx2^{Cre}$ mice, flexural rigidity and cortical thickness of the femurs were significantly increased, while the trabecular bone mass was not affected.

In contrast to the cortical bone phenotype found by our study, others observed a decrease in cortical bone mass which could be attributed to the used *Prx1*-Cre model, leading to a deletion of the ER α very early in skeletal stem cells [29]. No effects on either bone mass or composition were observed when using the *Col1a1*-Cre model to delete the ER α [29]. However, similar to our results, cortical bone mass and biomechanical strength was increased in male mice when ER α was deleted in mature osteoblasts and osteocytes (OC-Cre) [33]. However, these mice also displayed an increased femoral length as well as a significantly higher cancellous BV/TV and greater trabecular thickness at the tibial metaphysis [33]. Most likely, these differences are due to the different Cre model that was used. In other studies that also used the OC-Cre model, no cortical or trabecular changes were found in 16-week-old male mice [34] or in 26-week old mice [31], whereas in 24-week-old male mice, tibial BV/TV and TbN were lower [34]. However, the genetic background of those mice was not reported [34] while in the study of Melville and in our study, C57BL/6 mice were used. The genetic background can strongly influence bone structure and mass [44], which might explain these inconsistent results. A study by Windahl and colleagues analyzed the bone phenotype of male mice with an ER α deletion in osteocytes, showing that the trabecular bone volume was significantly reduced while cortical bone was unaffected [35]. The authors propose that the ER α in osteocytes is necessary to facilitate estrogen signaling that may result in an enhanced osteoblast activity which might explain the reduced trabecular bone phenotype due to a reduced osteoblast activity [35].

To draw conclusions about the role of the ER α on hypertrophic chondrocytes, we compare our results to the data generated under the *Col1a1*-Cre promotor, because it is known that *Col1a1* and *Runx2* are simultaneously upregulated in osteoblast precursors. *Runx2* is known to induce *Col1a1* gene expression in osteoblasts and is further expressed by transdifferentiating hypertrophic chondrocytes [41]. In contrast to the male *Col1a1*-Cre mice, which did not display any bone phenotype, we observe in our *Runx2*-Cre animals a significantly increased cortical thickness and a higher flexural rigidity. These differences suggest that in *Runx2*-Cre mice, the additional deletion of the ER α in hypertrophic chondrocytes might have a crucial impact on the bone phenotype, indicating that the ER α under physiological conditions might have a regulatory role on the transdifferentiation of hypertrophic chondrocytes into osteoblasts and that this process might contribute to cortical bone accrual in male mice. Another reason for the increased cortical thickness might be the involvement of ER α in the estrogen-dependent suppression of periosteal bone mass accrual

during bone development [1,5,33,45], which in addition might explain the higher cortical bone mass in male $ER\alpha^{fl/fl}; Runx2^{Cre}$ mice. Furthermore, testosterone might have a stronger positive impact on periosteal bone formation in male mice lacking $ER\alpha$ and possibly result in an increase in cortical thickness via androgen receptors [33]. These findings indicate that $ER\alpha$ mediates its effects on limiting periosteal expansion primarily during the stage of *Runx2*-positive osteoblast precursor cells, as well as during the *OC*-positive mature osteoblasts. In trabecular bone, the effect of $ER\alpha$ appears less prominent, because most of the studies do not report an altered trabecular bone microarchitecture in male mice.

$ER\alpha$ deletion in osteoblast progenitor cells and hypertrophic chondrocytes of female mice resulted in significant trabecular bone loss, whereas the bending stiffness of the femurs and the cortical thickness were unaltered.

When $ER\alpha$ deletion occurred at the stage of skeletal stem cells (*Prx1*-Cre) prior to *Runx2* expression, cortical bone mass and BMD were reduced in female mice, whereas the trabecular bone mass was unchanged [29]. Others demonstrated a significantly reduced trabecular bone mass in the tibiae and spine of female *Runx2*-Cre knockout mice aged 16 weeks, confirming our results [30]. By contrast, in the *Col1a1*-Cre model, no effect on cortical or trabecular bone was observed [29]. When $ER\alpha$ was deleted at the stage of pre-osteoblasts (*Osx1*-Cre), female mice displayed a reduced cortical thickness and unchanged trabecular bone parameters. Other studies that have used the *OC*-Cre model to delete the $ER\alpha$ in mature osteoblasts and osteocytes demonstrated that the trabecular bone mass was significantly reduced in female $ER\alpha$ -KO mice together with an altered cancellous architecture in the proximal tibia, distal femur, and L5 vertebral body [31–34]. Additionally, they observed a significant decrease in the cortical area and cortical thickness. Interestingly, the $ER\alpha$ on osteocytes was not required for maintaining both trabecular and cortical bone mass in female mice [35].

In comparison to the *Col1a1*-Cre model, which showed no bone phenotype, our data suggest that the decreased trabecular bone mass of the female $ER\alpha^{fl/fl}; Runx2^{Cre}$ mice results from the reduced number of trabecular osteoblasts that were also found to be significantly reduced in their surface, which is a surrogate for their activity. We hypothesize that the presence of the $ER\alpha$ on hypertrophic chondrocytes might be crucial for the transdifferentiation into osteoblasts that might participate in the formation of trabecular bone. However, future studies are needed to characterize the role of $ER\alpha$ in transdifferentiation of hypertrophic chondrocytes in more detail. Furthermore, we found that primary osteoblasts isolated from female $ER\alpha^{fl/fl}; Runx2^{Cre}$ displayed a significantly reduced differentiation ability. This finding is consistent with one study showing that $ER\alpha$ -deficient osteoblast progenitors from the periosteum have a decreased differentiation potential [29]. In cortical bone of the female $ER\alpha^{fl/fl}; Runx2^{Cre}$ mice, periosteal and endosteal diameters as well as osteocyte numbers were significantly reduced. These findings confirm that the $ER\alpha$ in osteoblast precursors is involved in endosteal bone resorption [46] and explain the reduced endosteal diameter. Regarding the reduced periosteal diameter, it is known that the $ER\alpha$ is important for periosteal bone apposition in female mice [29], resulting in a lower periosteal diameter when $ER\alpha$ is deleted. However, the molecular pathways behind these findings need to be addressed in further studies.

Taken together, the functions of $ER\alpha$ appear to be highly dependent on the maturation status of osteoblasts, while it starts to exert its positive effects on the trabecular bone of female mice at the stage of *Runx2*-positive osteoblast progenitor cells and is additionally required in mature osteoblasts, but not osteocytes. In cortical bone, $ER\alpha$ might be involved at very early stages of osteoblast maturation (*Prx1*-Cre) as well as in mature osteoblasts (*OC*-Cre) in female mice.

When the $ER\alpha$ was specifically deleted in chondrocytes by using a *Col2a1*-Cre model, no effects on skeletal growth or bone mineral density was reported [47] suggesting that the cartilage-specific $ER\alpha$ might not influence bone metabolism and structure. In our *Runx2*-Cre model, transdifferentiating chondrocytes and osteoblastic cells are affected by

the deletion and we observed a bone phenotype in both males and females, suggesting a sex-specific role of ER α in hypertrophic chondrocytes.

One limitation of our study is that we only analyzed the bone phenotype at the age of 12 weeks, whereas it would be of interest to also include also younger and older mice to investigate bone growth and development in more detail. Furthermore, to study the contribution of estrogen-dependent or -independent signaling to the observed bone phenotype in female ER $\alpha^{fl/fl}; Runx2^{Cre}$ mice, it would be of interest to investigate the bone response to ovariectomy in these mice.

In conclusion, we demonstrated that the ER α in osteoblast progenitors and hypertrophic chondrocytes is crucial for mediating anabolic effects on trabecular bone in female mice, whereas in males it has different effects by limiting the estrogen-dependent periosteal apposition in cortical bone. This suggests a sex-specific role of the ER α that is either promoting or repressing bone apposition at different sites of the long bones. The ER α in hypertrophic chondrocytes might be critically involved in the transdifferentiation towards osteoblasts, thereby regulating bone mass. These findings might be relevant also for human bone development, because case reports have already demonstrated the importance of estrogens and ER α signaling for human skeletal homeostasis [15–18].

4. Materials and Methods

4.1. Animal Care and Animal Models

All experiments were performed according to the ARRIVE guidelines and were approved by the local ethical committee (o.135-9, Regierungspräsidium Tübingen, Germany). Osteoblast progenitor cell-specific ER α -KO mice (Tg(Runx2-cre)1Jtuc x Esr1tm1.2Mma) were generated by crossing Runx2-Cre with ER $\alpha^{fl/fl}$ mice on a C57BL/6 background. ER $\alpha^{fl/fl}; Runx2^{Cre}$ mice were shown to lack the ER α in cells of the osteogenic lineage and in hypertrophic chondrocytes [48]. Age-matched, floxed littermates (ER $\alpha^{fl/fl}$) with no active Cre-transgene were used as control. All animals were housed in groups of up to five mice per cage with a 14-h light, 10-h dark rhythm and received water ad libitum as well as a standard mouse feed (ssniff R/M-H, V1535-300; Ssniff, Soest, Germany). At the age of 12 weeks, mice were sacrificed using an isoflurane overdose. Mouse genotyping was conducted by lysed tail PCR using the primers: 5'-CCA GGA AGA CTG CCA GAA GG-3', 5'-TGG CTT GCA GGT ACA GGA G-3' and 5'-GGA GCT GCC GAG TCA ATA AC-3' to detect the Cre transgene, whereas the ER α loxP sites were detected using the primers: 5'-TAG GCT TTG TCT CGC TTT CC-3', 5'-CCC TGG CAA GAT AAG ACA GC-3' and 5'-AGG AGA ATG AGG TGG CAC AG-3'.

4.2. Biomechanical Testing

To evaluate flexural rigidity of the femora, a non-destructive three-point bending test was performed on freshly prepared samples as described previously [49]. Briefly, an axial load with a maximum of 4 N was applied on the cranial side at the diaphyseal region of the bone using a material-testing machine (1454, Zwick GmbH & Co KG, Ulm, Germany). The flexural rigidity was calculated from the slope of the load-deflection curve.

4.3. μ CT Analysis

Femora were fixed in 4% phosphate-buffered formaldehyde solution and scanned using a μ CT scanning device (Skyscan 1172 v1.5; Skyscan, Kontich, Belgium) at a resolution of 8 μ m using a peak voltage of 50 kV and 200 μ A. Analyses and calibration steps were performed according to the guidelines of the American Society for Bone and Mineral Research [50] and volumes of interest were chosen as previously described [51]. Briefly, cortical bone was evaluated in a volume of interest (VOI) of 168 μ m length within the mid-diaphyseal region. The trabecular bone was assessed 200 μ m proximal of the metaphyseal growth plate over a length of 280 μ m in the distal femur, excluding the cortex. For assessing the epiphyseal femur, the trabecular bone was evaluated distal from the growth plate by a defined cylindrical VOI.

Within each scan, two phantoms with a defined density of hydroxyapatite (250 and 750 mg hydroxyapatite/cm³) were included to determine the bone mineral density. To distinguish between mineralized and nonmineralized tissue, thresholds for cortical bone (641.9 mg hydroxyapatite/cm³) and trabecular bone (394.8 mg hydroxyapatite/cm³) were used [52]. Analyses were performed by means of Skyscan software (NRecon v1.7.1.0, DataViewer v1.5.1.2, and CTAn v1.17.2.2).

4.4. Histomorphometry

Femora were fixed in 4% phosphate-buffered formaldehyde solution, decalcified using 20% EDTA (pH 7.2 to 7.4) for at least 14 days, and embedded in paraffin. The number and surface of osteoclasts was evaluated using tartrate-resistant alkaline phosphatase (TRAP) staining, whereas osteoblast number and surface were analyzed using Toluidine blue-stained sections. Osteoclasts were defined as TRAP-positive cells with two or more nuclei, directly located on the bone surface with a visible resorption lacunae between the bone surface and the cell. Osteoblasts were identified as cubic-shaped and Toluidine blue-positive cells with visible cytoplasm, directly located on the bone surface. Both osteoclasts and osteoblast parameters were evaluated at the femur metaphysis and normalized to bone surface using the Osteomeasure system (OsteoMeasure system v4.1.0.0; OsteoMetrics, Inc., Decatur, GA, USA). Growth plate thickness was analyzed in Safranin O-stained sections using the Osteomeasure system. Osteoclast activity at the growth plate was assessed within a defined region of 480 µm × 350 µm and osteoclasts were identified as multinucleated cells either laying directly on bone or cartilage tissue. Images were obtained using a Leica microscope (DMI 6000B). All analyses were performed according to American Society for Bone and Mineral Research standards [53].

4.5. Cultivation of Primary Mouse Osteoblasts

Primary osteoblasts were isolated from long bones of 12-week-old mice, as previously described [54]. Briefly, long bones were harvested, and bone marrow was flushed out by centrifugation. Bone diaphyses were cut into pieces and subjected to a 60-min collagenase digestion using 125 U/mL collagenase type VI (Sigma-Aldrich, Taufkirchen, Germany). For osteoblast expansion, bone chips were cultivated in modified minimal essential medium (DMEM; Biochrom, Berlin, Germany) containing, 1% l-glutamine (PAN-Biotech, Aidenbach, Germany), 100 U/mL penicillin/streptomycin, and 0.5% amphotericin B (Fungizone), supplemented with 15% fetal calf serum (all from Gibco, Darmstadt, Germany) at 37 °C under 5% CO₂. For the experiments, osteogenic differentiation was induced in the presence of 0.2 mmol/L ascorbate-2-phosphate and 10 mmol/L β-glycerophosphate (both from Sigma-Aldrich). Differentiation medium was replaced twice per week. Alkaline phosphatase stainings were performed by using a commercially available kit (Sigma-Aldrich) to confirm osteogenic differentiation after 14 days. In addition, mRNA samples were obtained after 10 days of osteogenic differentiation. Passage 2 osteoblasts were used for all experiments, which were performed in triplicates at least two times. The SensiFAST SYBR Hi-ROX One-Step Kit (Bioline, Memphis, TN, USA) was used according to the manufacturer's guidelines to perform quantitative PCR. B2M (F: 5'-ATACGCCTGCAGAGTTAAGCA-3', R: 5'-TCACAT GTCTCGATCCCAGT-3') was used as the housekeeping gene. Relative gene expression of AP (F: 5'-GCT GAT CAT TCC CAC GTT TT-3', R: 5'-GAG CCA GAC CAA AGA TGG AG-3'), OC (F: 5'-CTT GGT GCA CAC CTA GCA GA-3', R: 5'-ACC TTA TTG CCC TCC TGC TT-3'), BSP (F: 5'-GAA GCA GGT GCA GAA GGA AC-3', R: 5'-GAA ACC CGT TCA GAA GGA CA-3'), Runx2 (F: 5'-CCA CCA CTC ACT ACC ACA CG-3', R: 5'-CAC TCT GGC TTT GGG AAG AG-3'), Col1 (F: 5'-GCT GCA TAC ACA ATG GCC TA-3', R: 5'-TCA AGC ATA CCT CGG GTT TC-3'), and ERα (F: 5'-TCC GGC ACA TGA GTA ACA AA-3', R: 5'-CCA GGA GCA GGT CAT AGA GG-3') was calculated using the delta-delta CT method.

4.6. Statistics

Group size was $n = 6-8$ per group for bone phenotyping. Data were tested for normal distribution using the Shapiro–Wilk test; most data sets were normally distributed. Statistical testing was performed using t-tests with GraphPad Prism 8.4.3 (GraphPad Software, La Jolla, CA, USA). The level of significance was set at $p \leq 0.05$. Results are presented as box-and-whisker plots (with median and interquartile range) from maximum to minimum, showing all data points.

Supplementary Materials: The following are available online at <https://www.mdpi.com/article/10.3390/ijms23052902/s1>.

Author Contributions: Conceptualization, L.S., A.I. and M.H.-L.; methodology, L.S.; software, L.S.; validation, L.S. and J.B.; formal analysis, L.S.; investigation, L.S. and J.B.; resources, A.I. and M.H.-L.; data curation, L.S.; writing—original draft preparation, L.S.; writing—review and editing, A.I. and M.H.-L.; visualization, L.S.; supervision, A.I., J.T. and M.H.-L.; project administration, A.I., J.T. and M.H.-L.; funding acquisition, A.I. and M.H.-L. All authors have read and agreed to the published version of the manuscript.

Funding: This research was funded by the German Research Foundation (DFG, Project-ID HA 8470/1-1; 419) and by the Collaborative Research Center (CRC1149, Project-ID 251293561).

Institutional Review Board Statement: The animal study was protocol was approved by the local.

Informed Consent Statement: Ethical committee Regierungspräsidium Tübingen, Germany (o.135-9, 10 March 2020).

Data Availability Statement: Not applicable.

Acknowledgments: We thank Kristina Karremann, Tina Hieber, Andrea Böhmeler, and Iris Baum for excellent technical assistance.

Conflicts of Interest: The authors declare no conflict of interest. The funders had no role in the design of the study; in the collection, analyses, or interpretation of data; in the writing of the manuscript, or in the decision to publish the results.

References

- Riggs, B.L.; Khosla, S.; Melton, L.J. Sex steroids and the construction and conservation of the adult skeleton. *Endocr. Rev.* **2002**, *23*, 279–302. [[CrossRef](#)] [[PubMed](#)]
- Callewaert, F.; Sinnesael, M.; Gielen, E.; Boonen, S.; Vanderschueren, D. Skeletal sexual dimorphism: Relative contribution of sex steroids, GH-IGF1, and mechanical loading. *J. Endocrinol.* **2010**, *207*, 127–134. [[CrossRef](#)] [[PubMed](#)]
- Vanderschueren, D.; Laurent, M.R.; Claessens, F.; Gielen, E.; Lagerquist, M.; Vandenput, L.; Börjesson, A.E.; Ohlsson, C. Sex Steroid Actions in Male Bone. *Endocr. Rev.* **2014**, *35*, 906–960. [[CrossRef](#)] [[PubMed](#)]
- Khosla, S. Update on Estrogens and the Skeleton. *J. Clin. Endocrinol. Metab.* **2010**, *95*, 3569–3577. [[CrossRef](#)]
- Manolagas, S.C.; O'Brien, C.A.; Almeida, M. The role of estrogen and androgen receptors in bone health and disease. *Nat. Rev. Endocrinol.* **2013**, *9*, 699–712. [[CrossRef](#)]
- Callewaert, F.; Boonen, S.; Vanderschueren, D. Sex steroids and the male skeleton: A tale of two hormones. *Trends Endocrinol. Metab.* **2010**, *21*, 89–95. [[CrossRef](#)]
- Vanderschueren, D.; Vandenput, L.; Boonen, S.; Lindberg, M.K.; Bouillon, R.; Ohlsson, C. Androgens and Bone. *Endocr. Rev.* **2004**, *25*, 389–425. [[CrossRef](#)]
- Almeida, M.; Laurent, M.R.; Dubois, V.; Claessens, F.; O'Brien, C.A.; Bouillon, R.; Vanderschueren, D.; Manolagas, S.C. Estrogens and Androgens in Skeletal Physiology and Pathophysiology. *Physiol. Rev.* **2017**, *97*, 135–187. [[CrossRef](#)]
- Manolagas, S.C.; Bellido, T.; Jilka, R.L. Sex Steroids, Cytokines and the Bone Marrow: New Concepts on the Pathogenesis of Osteoporosis. *Physiol. Rev.* **2007**, *191*, 187–202. [[CrossRef](#)]
- Bord, S.; Horner, A.; Beavan, S.; Compston, J. Estrogen Receptors? and? Are Differentially Expressed in Developing Human Bone 1. *J. Clin. Endocrinol. Metab.* **2001**, *86*, 2309–2314. [[CrossRef](#)]
- Khalid, A.B.; Krum, S.A. Estrogen receptors alpha and beta in bone. *Bone* **2016**, *87*, 130–135. [[CrossRef](#)] [[PubMed](#)]
- Liu, M.-M.; Albanese, C.; Anderson, C.M.; Hilty, K.; Webb, P.; Uht, R.M.; Price, R.H.; Pestell, R.G.; Kushner, P.J. Opposing action of estrogen receptors α and β on cyclin D1 gene expression. *J. Biol. Chem.* **2002**, *277*, 24353–24360. [[CrossRef](#)] [[PubMed](#)]
- Lindberg, M.K.; Movérare, S.; Skrtic, S.; Gao, H.; Dahlman-Wright, K.; Gustafsson, J.-A.; Ohlsson, C. Estrogen Receptor (ER)- β Reduces ER α -Regulated Gene Transcription, Supporting a “Ying Yang” Relationship between ER α and ER β in Mice. *Mol. Endocrinol.* **2003**, *17*, 203–208. [[CrossRef](#)] [[PubMed](#)]

14. Smith, E.P.; Boyd, J.; Frank, G.R.; Takahashi, H.; Cohen, R.M.; Specker, B.; Williams, T.C.; Lubahn, D.B.; Korach, K. Estrogen Resistance Caused by a Mutation in the Estrogen-Receptor Gene in a Man. *N. Engl. J. Med.* **1994**, *331*, 1056–1061. [[CrossRef](#)]
15. Vanderschueren, D.; Van Herck, E.; Nijs, J.; Ederveen, A.G.H.; De Coster, R.; Bouillon, R. Aromatase Inhibition Impairs Skeletal Modeling and Decreases Bone Mineral Density in Growing Male Rats*. *Endocrinology* **1997**, *138*, 2301–2307. [[CrossRef](#)]
16. Vidal, O.; Lindberg, M.K.; Hollberg, K.; Baylink, D.J.; Andersson, G.; Lubahn, D.B.; Mohan, S.; Gustafsson, J.Å.; Ohlsson, C. Estrogen receptor specificity in the regulation of skeletal growth and maturation in male mice. *Proc. Natl. Acad. Sci. USA* **2000**, *97*, 5474–5479. [[CrossRef](#)]
17. Bouillon, R.; Bex, M.; Vanderschueren, D.; Boonen, S. Estrogens Are Essential for Male Pubertal Periosteal Bone Expansion. *J. Clin. Endocrinol. Metab.* **2004**, *89*, 6025–6029. [[CrossRef](#)]
18. Rochira, V.; Zirilli, L.; Madeo, B.; Aranda, C.; Caffagni, G.; Fabre, B.; Montangero, V.E.; Roldan, E.; Maffei, L.; Carani, C. Skeletal effects of long-term estrogen and testosterone replacement treatment in a man with congenital aromatase deficiency: Evidences of a priming effect of estrogen for sex steroids action on bone. *Bone* **2007**, *40*, 1662–1668. [[CrossRef](#)]
19. Gennari, L.; Merlotti, D.; Becherini, L.; Martini, G.; De Paola, V.; Calabrò, A.; Nuti, R. Estrogen Receptor Gene Polymorphisms and the Genetics of Osteoporosis: A HuGE Review. *Am. J. Epidemiol.* **2005**, *161*, 307–320. [[CrossRef](#)]
20. Sims, N.; Clément-Lacroix, P.; Minet, D.; Fraslou-Vanhulle, C.; Gaillard-Kelly, M.; Resche-Rigon, M.; Baron, R. A functional androgen receptor is not sufficient to allow estradiol to protect bone after gonadectomy in estradiol receptor-deficient mice. *J. Clin. Investig.* **2003**, *111*, 1319–1327. [[CrossRef](#)]
21. Haffner-Luntzer, M.; Fischer, V.; Ignatius, A. Differences in Fracture Healing Between Female and Male C57BL/6J Mice. *Front. Physiol.* **2021**, *12*, 2494. [[CrossRef](#)] [[PubMed](#)]
22. Somjen, D.; Katzburg, S.; Lieberherr, M.; Hendel, D.; Yoles, I. DT56a stimulates gender-specific human cultured bone cells in vitro. *J. Steroid Biochem. Mol. Biol.* **2006**, *98*, 90–96. [[CrossRef](#)] [[PubMed](#)]
23. Somjen, D.; Katzburg, S.; Sharon, O.; Knoll, E.; Hendel, D.; Stern, N. Sex specific response of cultured human bone cells to ER α and ER β specific agonists by modulation of cell proliferation and creatine kinase specific activity. *J. Steroid Biochem. Mol. Biol.* **2011**, *125*, 226–230. [[CrossRef](#)]
24. Couse, J.F.; Korach, K.S. Estrogen Receptor Null Mice: What Have We Learned and Where Will They Lead Us? *Endocr. Rev.* **1999**, *20*, 358–417. [[CrossRef](#)] [[PubMed](#)]
25. Vidal, O.; Lindberg, M.; Sävendahl, L.; Lubahn, D.; Ritzen, E.; Gustafsson, J.; Ohlsson, C. Disproportional Body Growth in Female Estrogen Receptor- α -Inactivated Mice. *Biochem. Biophys. Res. Commun.* **1999**, *265*, 569–571. [[CrossRef](#)]
26. Lindberg, M.K.; Alatalo, S.L.; Halleen, J.M.; Mohan, S.; Gustafsson, J.; Ohlsson, C. Estrogen receptor specificity in the regulation of the skeleton in female mice. *J. Endocrinol.* **2001**, *171*, 229–236. [[CrossRef](#)] [[PubMed](#)]
27. Sims, N.; Dupont, S.; Krust, A.; Clement-Lacroix, P.; Minet, D.; Resche-Rigon, M.; Gaillard-Kelly, M.; Baron, R. Deletion of estrogen receptors reveals a regulatory role for estrogen receptors- β in bone remodeling in females but not in males. *Bone* **2002**, *30*, 18–25. [[CrossRef](#)]
28. Couse, J.F.; Curtis, S.W.; Washburn, T.F.; Golding, T.S.; Lubahn, D.B.; Korach, K.S.; Lindzey, J.; Smithies, O. Analysis of transcription and estrogen insensitivity in the female mouse after targeted disruption of the estrogen receptor gene. *Mol. Endocrinol.* **1995**, *9*, 1441–1454. [[CrossRef](#)]
29. Almeida, M.; Iyer, S.; Martin-Millan, M.; Bartell, S.M.; Han, L.; Ambrogini, E.; Onal, M.; Xiong, J.; Weinstein, R.S.; Jilka, R.L.; et al. Estrogen receptor- α signaling in osteoblast progenitors stimulates cortical bone accrual. *J. Clin. Investig.* **2012**, *123*, 394–404. [[CrossRef](#)]
30. Seitz, S.; Keller, J.; Schilling, A.F.; Jeschke, A.; Marshall, R.P.; Stride, B.D.; Wintermantel, T.; Beil, F.T.; Amling, M.; Schutz, G.; et al. Pharmacological Estrogen Administration Causes a FSH-Independent Osteo-Anabolic Effect Requiring ER Alpha in Osteoblasts. *PLoS ONE* **2012**, *7*, e50301. [[CrossRef](#)]
31. Rooney, A.M.; Ayobami, O.O.; Kelly, N.H.; Schimenti, J.C.; Ross, F.P.; van der Meulen, M.C. Bone mass and adaptation to mechanical loading are sexually dimorphic in adult osteoblast-specific ER α knockout mice. *Bone* **2022**, *158*, 116349. [[CrossRef](#)] [[PubMed](#)]
32. Melville, K.M.; Kelly, N.H.; Khan, S.; Schimenti, J.C.; Ross, F.P.; Main, R.P.; van der Meulen, M.C.H. Female Mice Lacking Estrogen Receptor-Alpha in Osteoblasts Have Compromised Bone Mass and Strength. *J. Bone Miner. Res.* **2013**, *29*, 370–379. [[CrossRef](#)] [[PubMed](#)]
33. Melville, K.M.; Kelly, N.H.; Surita, G.; Buchalter, D.B.; Schimenti, J.C.; Main, R.P.; Ross, F.P.; Van Der Meulen, M.C.H. Effects of Deletion of ER α in Osteoblast-Lineage Cells on Bone Mass and Adaptation to Mechanical Loading Differ in Female and Male Mice. *J. Bone Miner. Res.* **2015**, *30*, 1468–1480. [[CrossRef](#)]
34. Määttä, J.A.; Büki, K.G.; Gu, G.; Alanne, M.H.; Vääräniemi, J.; Liljenbäck, H.; Poutanen, M.; Härkönen, P.; Väänänen, K. Inactivation of estrogen receptor α in bone-forming cells induces bone loss in female mice. *FASEB J.* **2012**, *27*, 478–488. [[CrossRef](#)] [[PubMed](#)]
35. Windahl, S.H.; Borjesson, A.E.; Farman, H.H.; Engdahl, C.; Moverare-Skrtic, S.; Sjögren, K.; Lagerquist, M.; Kindblom, J.; Koskela, A.; Tuukkanen, J.; et al. Estrogen receptor- in osteocytes is important for trabecular bone formation in male mice. *Proc. Natl. Acad. Sci. USA* **2013**, *110*, 2294–2299. [[CrossRef](#)] [[PubMed](#)]
36. Miron, R.J.; Zhang, Y.F. Osteoinduction: A review of old concepts with new standards. *J. Dent. Res.* **2012**, *91*, 736–744. [[CrossRef](#)]

37. Park, J.; Gebhardt, M.; Golovchenko, S.; Perez-Branguli, F.; Hattori, T.; Hartmann, C.; Zhou, X.; Decrombrugge, B.; Stock, M.; Schneider, H.; et al. Dual pathways to endochondral osteoblasts: A novel chondrocyte-derived osteoprogenitor cell identified in hypertrophic cartilage. *Biol. Open* **2015**, *4*, 608–621. [[CrossRef](#)]
38. Bruderer, M.; Richards, R.G.; Alini, M.; Stoddart, M.J. Role and regulation of RUNX2 in osteogenesis. *Eur. Cell Mater.* **2014**, *28*, 269–286. [[CrossRef](#)]
39. Zhou, X.; Von Der Mark, K.; Henry, S.; Norton, W.; Adams, H.; De Crombrugge, B. Chondrocytes Transdifferentiate into Osteoblasts in Endochondral Bone during Development, Postnatal Growth and Fracture Healing in Mice. *PLoS Genet.* **2014**, *10*, e1004820. [[CrossRef](#)]
40. Hu, D.P.; Ferro, F.; Yang, F.; Taylor, A.J.; Chang, W.; Miclau, T.; Marcucio, R.S.; Bahney, C.S. Cartilage to bone transformation during fracture healing is coordinated by the invading vasculature and induction of the core pluripotency genes. *Development* **2017**, *144*, 221–234. [[CrossRef](#)]
41. Ducy, P.; Zhang, R.; Geoffroy, V.; Ridall, A.L.; Karsenty, G. *Osf2/Cbfa1*: A Transcriptional Activator of Osteoblast Differentiation. *Cell* **1997**, *89*, 747–754. [[CrossRef](#)]
42. Otto, F.; Thornell, A.P.; Crompton, T.; Denzel, A.; Gilmour, K.C.; Rosewell, I.R.; Stamp, G.W.; Beddington, R.S.; Mundlos, S.; Olsen, B.R.; et al. *Cbfa1*, a Candidate Gene for Cleidocranial Dysplasia Syndrome, Is Essential for Osteoblast Differentiation and Bone Development. *Cell* **1997**, *89*, 765–771. [[CrossRef](#)]
43. Komori, T.; Yagi, H.; Nomura, S.; Yamaguchi, A.; Sasaki, K.; Deguchi, K.; Shimizu, Y.; Bronson, R.; Gao, Y.-H.; Inada, M.; et al. Targeted Disruption of *Cbfa1* Results in a Complete Lack of Bone Formation owing to Maturational Arrest of Osteoblasts. *Cell* **1997**, *89*, 755–764. [[CrossRef](#)]
44. Sabsovich, I.; Clark, J.D.; Liao, G.; Peltz, G.; Lindsey, D.P.; Jacobs, C.R.; Yao, W.; Guo, T.-Z.; Kingery, W.S. Bone microstructure and its associated genetic variability in 12 inbred mouse strains: μ CT study and in silico genome scan. *Bone* **2008**, *42*, 439–451. [[CrossRef](#)] [[PubMed](#)]
45. Turner, R.T.; Colvard, D.S.; Spelsberg, T.C. Estrogen Inhibition of Periosteal Bone Formation in Rat Long Bones: Down-Regulation of Gene Expression for Bone Matrix Proteins*. *Endocrinology* **1990**, *127*, 1346–1351. [[CrossRef](#)]
46. Emmanuelle, N.E.; Marie-Cécile, V.; Florence, T.; Jean-François, A.; Françoise, L.; Coralie, F.; Alexia, V. Critical role of estrogens on bone homeostasis in both male and female: From physiology to medical implications. *Int. J. Mol. Sci.* **2021**, *22*, 1–18.
47. Börjesson, A.; Lagerquist, M.K.; Liu, C.; Shao, R.; Windahl, S.H.; Karlsson, C.; Sjögren, K.; Movérare-Skrtic, S.; Antal, M.C.; Krust, A.; et al. The role of estrogen receptor α in growth plate cartilage for longitudinal bone growth. *J. Bone Miner. Res.* **2010**, *25*, 2690–2700. [[CrossRef](#)]
48. Steppe, L.; Krüger, B.T.; Tschaffon, M.E.A.; Fischer, V.; Tuckermann, J.; Ignatius, A.; Haffner-Luntzer, M. Estrogen Receptor α Signaling in Osteoblasts is Required for Mechanotransduction in Bone Fracture Healing. *Front. Bioeng. Biotechnol.* **2021**, *9*, 2355. [[CrossRef](#)]
49. Röntgen, V.; Blakytyn, R.; Matthys, R.; Landauer, M.; Wehner, T.; Göckelmann, M.; Jermendy, P.; Amling, M.; Schinke, T.; Claes, L.; et al. Fracture healing in mice under controlled rigid and flexible conditions using an adjustable external fixator. *J. Orthop. Res.* **2010**, *28*, 1456–1462. [[CrossRef](#)]
50. Bouxsein, M.L.; Boyd, S.K.; Christiansen, B.A.; Guldborg, R.E.; Jepsen, K.J.; Müller, R. Guidelines for assessment of bone microstructure in rodents using micro-computed tomography. *J. Bone Miner. Res.* **2010**, *25*, 1468–1486. [[CrossRef](#)]
51. Haffner-Luntzer, M.; Kemmler, J.; Heidler, V.; Prystaz, K.; Schinke, T.; Amling, M.; Kovtun, A.; Rapp, A.E.; Ignatius, A.; Liedert, A. Inhibition of Midkine Augments Osteoporotic Fracture Healing. *PLoS ONE* **2016**, *11*, e0159278. [[CrossRef](#)] [[PubMed](#)]
52. Morgan, E.F.; Mason, Z.D.; Chien, K.B.; Pfeiffer, A.J.; Barnes, G.L.; Einhorn, T.; Gerstenfeld, L.C. Micro-computed tomography assessment of fracture healing: Relationships among callus structure, composition, and mechanical function. *Bone* **2009**, *44*, 335–344. [[CrossRef](#)] [[PubMed](#)]
53. Dempster, D.W.; Compston, J.E.; Drezner, M.K.; Glorieux, F.H.; Kanis, J.A.; Malluche, H.; Meunier, P.J.; Ott, S.M.; Recker, R.R.; Parfitt, A.M. Standardized nomenclature, symbols, and units for bone histomorphometry: A 2012 update of the report of the ASBMR Histomorphometry Nomenclature Committee. *J. Bone Miner. Res.* **2013**, *28*, 2–17. [[CrossRef](#)] [[PubMed](#)]
54. Rapp, A.E.; Bindl, R.; Recknagel, S.; Erbacher, A.; Müller, I.; Schrezenmeier, H.; Ehrnthaller, C.; Gebhard, F.; Ignatius, A. Fracture Healing Is Delayed in Immunodeficient NOD/scid-IL2R γ null Mice. *PLoS ONE* **2016**, *11*, e0147465. [[CrossRef](#)]